Physica B 517 (2017) 47–52

Contents lists available at ScienceDirect

Physica B

journal homepage: www.elsevier.com/locate/physb

Electronic structure of carbon antisite in SiC: localization versus delocalization

T.L. Petrenko*, V.P. Bryksa

Institute of Semiconductor Physics, NASU, 45 Prospect Nauky, 03028 Kyiv, Ukraine

ARTICLE INFO

Keywords:
SiC
Carbon antisite
Small polaron
Self interaction error

ABSTRACT

In paper (Baranov et al., 2008 [26]) the EPR spectrum with large ^{13}C isotope hyperfine splitting was observed in neutron-irradiated 6*H*-SiC crystals and attributed to the positively charged carbon antisite C_{Si}^{+}. However up till now numerous ab initio calculations show that this defect is optically and electrically inactive and hence it cannot be detected in experiment. In the present paper we have considered carbon antisite in framework of DFT with self interaction correction. We show that small polaron-like ground state with broken bond configuration may be formed in the case of positively charged carbon antisite C_{Si}^{+} while for negatively charged defect formation of such state is energy-unprofitable. For unambiguous identification of carbon antisite the parameters of hyperfine interaction with central carbon C_{Si} as well as with four nearest carbons were calculated and compared with EPR experiment both for positively and negatively charged centers.

1. Introduction

Together with vacancies and interstitials in binary semiconductors the antisites, appeared when atom of one sublattice occupies position in other sublattice, are among the simplest possible native defects. Such defects may be observed both in isolated form or as precursors of more complex defects and are of fundamental importance in semiconductor physics. Equilibrium concentration of antisite defects obtained during growth process is often negligibly small due to high value of formation energy. However such defects may be created in sufficient concentrations upon irradiation with near-threshold energy [1,2].

In recent years it was suggested that native defects in SiC polytypes are promising objects for quantum computing [3–5]. Nevertheless in many cases electronic structure of such defects remains controversial [6–8,5] though during last two decades the enormous progress was achieved in the field of intrinsic defects identification in SiC. The generally accepted method for this purpose consists in comparison of calculated (DFT) and measured (EPR or ENDOR techniques) parameters of hyperfine interaction with ^{29}Si and ^{13}C magnetic isotopes [9].

In such a way a number of simplest intrinsic defects and their complexes in various charge and spin states were identified in SiC polytypes. In particular, formation of silicon and carbon monovacancies [10–13], carbon split-interstitial [14], dicarbon antisite $(C_2)_{Si}$ [15] and divacancies [16] in various charge states was unambiguously proved due to excellent agreement of calculated hyperfine tensors with experimental ones.

For another simplest native defects - isolated antisites Si_C and C_{Si} situation is more complex and up till now none of them was identified with confidence (see, e.g. discussion in [6]). Only antisite containing native complex C_{Si}-V_C was observed [17] as a product of transformation of silicon vacancy which is known as metastable defect [18].

There is a number of papers which utilize DFT-based calculations to predict the formation energy and properties of carbon antisite C_{Si} in SiC since 1988 [19–23]. All of them use a plane-wave pseudopotential method, LSDA functional and supercells from 32 to 216 atoms, or numerical atomic-like basis [24]. In general these calculations agree one with another and predict that antisite C_{Si} exist only in the neutral charge state without energy levels in the gap. It has the T_d point symmetry with inward relaxation and the lowest formation energy among other native defects. However experimental observation of such defect is difficult because it is optically and electrically inactive and cannot manifest itself in magnetic resonance experiments. In addition it was argued that carbon antisite may be activated after trapping of interstitial hydrogen or other mobile defects [25].

Identification of dicarbon antisites $(C_2)_{Si}$ by means of EPR techniques and ab initio calculations [15] may serve as indirect evidence of existing the C_{Si} antisite as the precursor which traps the interstitial carbon. The reaction involving these defects was formerly predicted to be energetically favored in SiC [24].

In [26] EPR spectrum with axial g-tensor and large axial hyperfine splitting due to interaction with one carbon nucleus in ^{13}C isotope enriched neutron-irradiated and annealed 6*H*-SiC was reported.

* Corresponding author.
E-mail address: petrenkotl@isp.kiev.ua (T.L. Petrenko).

http://dx.doi.org/10.1016/j.physb.2017.05.005
Received 17 November 2016; Received in revised form 29 April 2017; Accepted 3 May 2017
Available online 04 May 2017

Authors speculated that such strong hyperfine interaction may be assigned to the central carbon of the positively charged C_{Si} antisite, while interaction with other coordinative shells produces the relatively broad unresolved lines hidden under the central part of spectrum. The proposed microscopic model resemble the broken bond configuration geometry similar to the one for As_{Ga} antisite in GaAs [27–29]. However this model sharply contradicts all performed earlier ab initio calculations.

We stress that there is not enough spin Hamiltonian parameters presented in [26] for rigorous identification of carbon antisite in SiC (actually it is very difficult experimental task). In fact authors implicitly use results of DFT calculations to reject e.g. the V_{Si} or C_{Si}-V_C models. For this reason we use designation C_X through the paper for unknown nucleus with hyperfine interaction observed in [26]. Therefore proper modeling of C_{Si} defect in various charge states is of crucial importance for unambiguous identification of C_X as C_{Si} nucleus.

If broken bond model [26] for carbon antisite is valid then one may expect that eliminating of self interaction error (SIE) is necessary to describe a hole or electron localization [30,31]. In this case going beyond local and semilocal approximations for exchange-correlation functionals is of crucial importance. The reason is that the exact total energy of a separated open system must depend linearly on a fraction charges between adjacent integers [32,33]. At the same time the energy dependence predicted by semilocal density functionals is concave up while the exact-exchange-only (Hartree-Fock) energy is concave down. As a result, local and semilocal functionals overestimate *delocalization* while Hartree-Fock calculations overestimate *localization*. Therefore one obvious way of eliminating the delocalization error is using of hybrid functionals containing some amount of exact exchange. In this case cancellation of errors occurs leading to nearly linear dependence of energy versus fractional charge. Unfortunately fraction of Hartree-Fock exchange (HFX) varies in wide range in different functionals and ”best” value depends on the considered problem. For example, the B3LYP hybrid adequately describe localization in the case of B^0_{Si} center in SiC [34] while it fails for Al_{Si} in SiO_2 [35] where at least 50% of HFX is necessary to obtain agreement with experiment. Thus it is difficult to perform *predictive* calculations using hybrid functionals. Review of modern methods which eliminate the delocalization error one may find in [36].

In [37] the self-interaction-corrected (SIC) DFT approach for spin-1/2 defects was proposed. This method is computationally inexpensive compared to hybrid functionals and was successfully validated in the case of famous prototype defect - Al_{Si} impurity in quartz with self-trapped hole which was a challenge for DFT during a long time.

The paper is organized as follows. In Section 2 we describe methods used for calculations. In Section 3 we present calculated potential energy curves depending on the C-C distance for a number of Hamiltonians accounting for self interaction error in a different ways to obtain the ground state structure of carbon antisite. In Section 4 we present calculations of hyperfine parameters and compare its values with experimental ones.

2. Method and details of calculation

Periodic DFT calculations employing cubic 64 and 216-atoms supercells (SC) were performed using the CP2K code [38]. This code utilize a Gaussian basis set and the density is represented in a plane wave auxiliary basis, or equivalently, on an equidistant grid in real space. The charge density was expanded in plane waves with a cutoff equal to 300 Ry. In CP2K code grids with different mesh sizes (or multigrids), are employed to compute matrix elements and densities [39] and we use relative cutoff parameter of 50 Ry for multigrid characterization.

We applied a double-ζ basis sets which include polarization *d*-functions as well [40]. The core electrons were described with the Goedecker-Teter-Hutter (GTH) pseudopotentials [41].

For calculations with hybrid functionals and 64-atoms SC we used truncated Coulomb operator [42] with cutoff radius of 4.0 Å (which is nearly one half of cubic cell dimension) together with the auxiliary density matrix method (ADMM) [43]. These two approaches greatly reduces the computational time necessary for computations involving nonlocal HFX.

All-electron calculation of hyperfine interaction tensor with ^{13}C isotope was performed in cluster approximation using ORCA code [44]. For the simulations of carbon antisite C_{Si} in 3C-SiC, we used the Si-centered tetrahedral cluster $C_{Si}Si_{42}C_{44}H_{76}$ (163 atoms), where broken bonds on the surface are saturated with hydrogens. Balanced gaussian basis sets [45] of triple zeta valence (def2-TZVP) with eliminated polarization *f*-functions and split valence (def2-SVP) quality were used. The first one was employed for central carbon C_{Si} together with four nearest carbons containing major part of spin density, while the second one - for the rest of cluster. In addition the TZVP basis set for carbon atom containing maximum of spin density was augmented with diffuse function for correct description of spin density in the broken bond region.

Cluster calculations with hybrid density functional BHandHLYP were performed using the resolution of identity (RI-J) algorithm for the evaluation of the Coulomb term, and efficient ‘chain of spheres exchange’ (COSX) algorithm for the calculation of the exchange terms [46]. For the fitting basis in the RI-J treatment, the ‘def2’ fit bases optimized for the SV and TZV basis sets were used [47].

Positions of all atoms in the cluster including the capped bond hydrogens, were optimized without symmetry constraints. The hyperfine tensors were calculated using the standard relations (see, e.g., [48]).

3. Localized and delocalized states of positively and negatively charged carbon antisites: crucial role of self interaction error

Considered broken bond model of charged C_{Si} carbon antisite together with used designations is shown in Fig. 1. In Figs. 2 and 3 results of relaxed surface scans are presented depending on the used level of theory and charge state of defect. To decrease magnitude of SIE we choose hybrid BHandHLYP functional containing 50% of HFX, GGA PBE functional with SIC [37] and Hartree-Fock method (100% HFX without correlation part). The first and second methods reduces the SIE, while the latter one is essentially self-interaction free. In addition we use popular hybrid functionals PBE0 and B3LYP containing relatively small amount of HFX (25% and 20%, respectively)

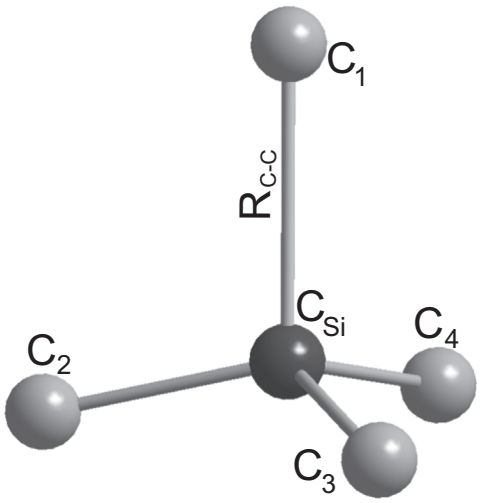

Fig. 1. Broken bond model for charged carbon antisite in SiC. Elongated (broken) bond C_{Si}-C_1 contains major part of spin density and other three bonds are shortened.

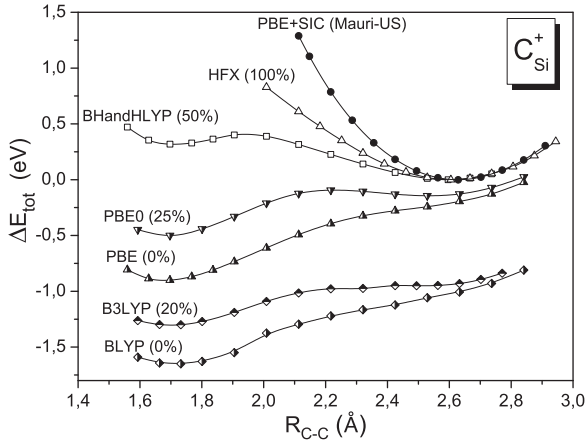

Fig. 2. Total energy versus C_{Si}-C_1 distance R_{CC} (see Fig. 1) for positively charged carbon antisite C^{+}_{Si} in 3*C*-SiC calculated using 64-atoms SCs at various levels of theory. Fraction of exact exchange inherent for particular functional is indicated in parentheses.

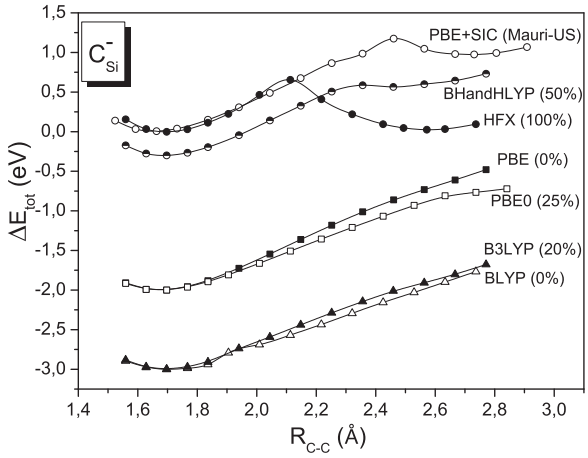

Fig. 3. Total energy versus C_{Si}-C_1 distance R_{CC} (see Fig. 1) for negatively charged carbon antisite C^{-}_{Si} in 3*C*-SiC calculated using 64-atoms SCs at various levels of theory. Fraction of exact exchange inherent for particular functional is indicated in parentheses.

together with corresponding GGA counterparts, namely PBE and BLYP functionals for comparison.

In the case of C^{+}_{Si} defect (Fig. 2) one can see that BHandHLYP, HFX and PBE+SIC approximations with reduced SIE lead to small polaron-like ground state with the hole localization on the C_{Si}-C_1 bond which is elongated up to 2.7 Å. At BHandHLYP level we found the additional local minimum which corresponds to the nearly regular tetrahedron $C_{Si}C_{1\div4}$ with $R_{CC} \simeq 1.7$ Å and delocalized hole.

At HFX and PBE+SIC levels of theory with the use of 64-atoms supercell we get instead the local minimum corresponding to the slightly deformed tetrahedron with the hole localized on the C_1-Si bond and C_s point symmetry. However calculations using the 216-atoms supercell show that such solution become unstable and spurious. In this case regular tetrahedron $C_{Si}C_{1\div4}$ and spin density spreaded over supercell were obtained for local minimum as well.

In Tables 1 and 3 local geometries in the vicinity of C^{+}_{Si} and C^{-}_{Si} centers depending on the functional and model system (cluster or supercell) used for calculations are presented.

One can see that all data in Table 1 may be divided into two groups. The first one corresponds to nearly regular geometry of tetrahedron $C_{Si}C_{1-4}$ which results from calculations with relatively large amount of SIE (BLYP, B3LYP, PBE and PBE0). The second group corresponds to strongly deformed tetrahedron which is inherent for methods with reduced SIE (HFX, BHandHLYP and PBE+SIC). In both cases there are four symmetry equivalent orientation of ⟨111⟩-type center axis and

Table 1
Ground state local geometry for C^{+}_{Si} carbon antisite in 3*C*-SiC calculated at various levels of theory. Supercells (SC) and clusters (CL) are model systems used for defect calculation. R_S denotes shortened bonds C_{Si}-$C_{2\div4}$ and R_L is elongated C_{Si}-C_1 bond as shown in Fig. 1.

Functional	Model system/ No of atoms	R_S (Å)	R_L (Å)
PBE+SIC	SC/64	1.516	2.630
PBE+SIC	SC/216	1.515	2.602
BHandHLYP	SC/64	1.537	2.596
BHandHLYP	CL/163	1.520	2.714
HFX	SC/64	1.545	2.606
HFX	CL/163	1.532	2.760
PBE0	SC/64	1.649	1.698
PBE	SC/64	1.649	1.697
B3LYP	SC/64	1.662	1.732
BLYP	SC/64	1.666	1.732

corresponding four equivalent minima. However motion of the system between such minima shows qualitatively different behavior. To elucidate differences we estimate position of saddle point in 64-atoms SC as midway between two equivalent minima designated as *a* and *b*:

$$\vec{r}_{i,s} = \frac{\vec{r}_{i,a} + \vec{r}_{i,b}}{2}, \quad i = 1 \div 64 \tag{1}$$

where $\vec{r}_{i,s}$, $\vec{r}_{i,a}$ and $\vec{r}_{i,b}$ are radius-vectors of i-th atom in SC for saddle point, minimum *a* and *b*, respectively. Such estimation is very close to exact transition state and give upper bound for reorientation barrier height ΔE_b [34]. For example at B3LYP level for C^{+}_{Si} center we obtain $\Delta E_b \leq 0.028$ eV. Besides this barrier is extremely narrow. Namely, movement of system from minimum to saddle point is accompanied with maximal atomic displacement of 0.026 Åonly. Thus calculations at B3LYP level of theory predict the motionally averaged delocalized ground state with regular tetrahedron $C_{Si}C_{1-4}$.

In contrast similar calculations with BHandHLYP hybrid functional give value of $\Delta E_b \leq 1.11$ eV with maximal atomic displacement of 0.38 Å when system moves from minimum to saddle point. This give grounds for identification of C^{+}_{Si} as small bound polaron or in other terms as the Jahn-Teller center with structure very similar to the isoelectronic B^{0}_{Si} defect in SiC [34].

In Table 2 energy differences between localized and delocalized states of carbon antisite calculated at various levels of theory and defect charges are listed.

It is seen that calculations with reduced SIE for C^{+}_{Si} carbon antisite support the small polaron defect model with large local lattice relaxation - elongating of C_{Si}-C_1 bond up to 2.7 Å and shortening of C_{Si}-C_{2-4} bonds down to 1.5 Å compared to 1.89 Å for Si-C distance in host crystal. We expect that this defect is electrically active and must manifest itself in magnetic resonance and optical experiments. However situation is more complex in the case of negatively charged carbon antisite C^{-}_{Si} as one can see from Fig. 3 and Table 2. Firstly, high value of exact exchange fraction (50%) in BHandHLYP functional do

Table 2
Relative energies of localized small polaron (E_{sp}) and delocalized (E_{deloc}) states for C_{Si} carbon antisite in 3*C*-SiC calculated at various levels of theory and defect charges.

Method	Defect charge	E_{deloc}-E_{sp} (eV)
BHandHLYP	+1	0.26
HFX	+1	0.64
PBE+SIC	+1	1.06
PBE+SIC[a]	+1	3.03
BHandHLYP	−1	−0.86
HFX	−1	0.025
PBE+SIC	−1	−0.97
PBE+SIC[a]	−1	−0.49

PBE+SIC[a] designation corresponds to calculation with 216 atoms supercell, while in all other calculations 64 atoms supercells were used.

Table 3
Ground state local geometries for C^{-}_{Si} carbon antisite in 3C-SiC calculated at various levels of theory.

Functional	Model system/ No of atoms	R_S (Å)	R_L (Å)
PBE+SIC	SC/64	1.655	1.663
PBE+SIC	SC/216	1.652	1.655
BHandHLYP	SC/64	1.678	1.681
BHandH*	CL/163	1.574	2.656
BHandH*	SC/64	1.599	2.460
HFX	SC/64	1.606	2.573
HFX	CL/163	1.574	2.720
PBE0	SC/64	1.658	1.670
PBE	SC/64	1.656	1.672
B3LYP	SC/64	1.679	1.682
BLYP	SC/64	1.678	1.696

Supercells (SC) and clusters (CL) are model systems used for defect calculation. R_S denotes shortened bonds C_{Si}- and R_L is elongated C_{Si}-C_1 bond as shown in Fig. 1. Designation BHandH* corresponds to the metastable state with broken bond configuration.

not lead to formation of small bound polaron. Secondly, SIC proposed in Ref. [37] must be used in this case with care because it is based on the restricted open shell formalism (ROKS) which is unable to describe the spin polarization effects, in particular existence of negative spin densities. However in the next section we will show that there are noticeable negative spin densities on the off-axis atoms $C_{2\div4}$. At the same time for positively charged antisite it is not so which explains the success of application of SIC [37] in this case.

From Fig. 3 and Table 2 one may see that only in the case of Hartree-Fock calculations the ground state of negatively charged carbon antisite corresponds to small polaron broken bond model. Nevertheless energy gain is very small (0.025 eV) while more reliable calculations using BHandHLYP hybrid functional show the 0.86 eV energy gain for delocalized state.

Besides from Table 3 one can see that with the exception of Hartree-Fock method the ground state geometries for C^{-}_{Si} center show the negligibly small deviations from tetrahedral symmetry. In particular elongated (R_L) and shortened (R_S) C_{Si}-$C_{1\div4}$ bonds differ only by ~0.01 Å. As a consequence no localization of spin density is obtained for negative charge state and small bound polaron in this case may be possibly formed only as a metastable defect. However experimental conditions described in [26] correspond to formation of stable defect rather than of metastable one (neutron irradiation at room temperature and subsequent isochronal annealing at temperatures up to 900 °C). Therefore we conclude that for negative carbon antisite C^{-}_{Si} delocalized state is preferable.

We note that all calculations which use GGA PBE and BLYP functionals together with corresponding PBE0 and B3LYP hybrids with relatively small amount of exact exchange give the delocalized states with nearly regular C_{Si}-$C_{1\div4}$ tetrahedron both for positive and negative carbon antisites. This is in line with numerous earlier calculations which predict that carbon antisite is electrically inactive defect.

4. Calculation of hyperfine parameters for carbon antisite and comparison with EPR experiment

For identification of carbon antisite we performed calculations of isotropic a_{iso} and anisotropic b parameters of hyperfine interaction with carbon atoms shown in Fig. 1 for C^{+}_{Si} antisite defect and compare with experiment [26]. Anisotropic constant b is defined as $b = T_{zz}/2$ where T_{ij} is traceless tensor of hyperfine interaction. Deviation of tensor from axial symmetry may be characterized by parameter $b' = (T_{xx} - T_{yy})/2$ which in all considered cases is small and hence may be neglected.

We choose hybrid BHandHLYP functional (which include 50% of exact exchange) for calculation of hyperfine parameters because it properly describes hole localization as is seen from Fig. 2. In addition we note that hybrid functionals in combination with cluster approximation usually show good results for calculation of spin density and spin Hamiltonian parameters [13,34].

Results of calculations for positively charged carbon antisite C^{+}_{Si} are presented in Fig. 4. It is seen that there is only one carbon atom containing major part of spin density leading to large hyperfine splitting observed in EPR spectrum [26] and speculatively attributed to the central carbon C_{Si} (see Fig. 1). However our calculations reveal that maximum of spin density and largest hyperfine splitting corresponds to hyperfine interaction with broken bond on-axis C_1 nucleus. Rough estimation of peak-to-peak line width from Fig. 2 in Ref. [26] gives value of $\Delta H_{pp} \approx 15$ MHz. Therefore EPR technique in principle cannot resolve hyperfine interaction with C_{Si} and C_{2-4} nuclei and more precise methods like ENDOR must be applied for this purpose.

It is worth to note that in spite of qualitative agreement with experiment (see hyperfine parameters for C_1 and C_X in Fig. 4*a*) the quantitative matching is not perfect. Indeed, our calculations overestimate p-character of wave function on C_1 and underestimate the s-character. The situation is somewhat similar to the center B^{0}_{Si} (which is isoelectronic to the C^{+}_{Si} one). In this case calculations with the use of a number of popular hybrid functionals overestimate p-character and underestimate the s-character on the on-axis carbon atom containing

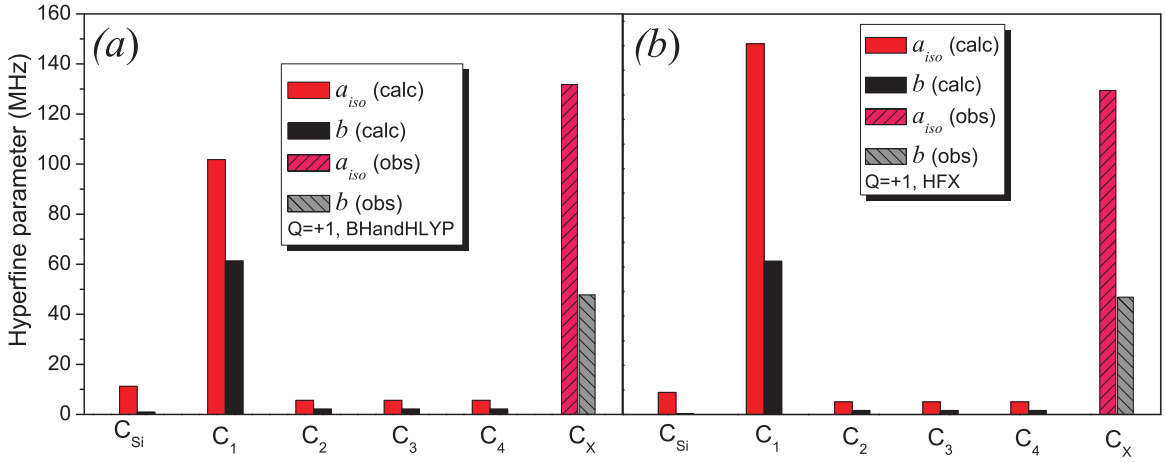

Fig. 4. *a*) Hyperfine parameters calculated using cluster approximation and BHandHLYP level of theory for C^{+}_{Si} carbon antisite. Labelling of atoms corresponds to designations in Fig. 1. Values of a_{iso}(obs) and b(obs) are parameters observed in [26] due to hyperfine interaction with one ^{13}C nucleus labelled as C_X; *b*) - the same but calculations were performed at Hartree-Fock level of theory.

major part of spin density as well [34].

To estimate influence of exchange part of used functional on the calculated hyperfine parameters we performed test calculations at the Hartree- Fock level of theory (100% of exact exchange without correlation part) shown in Fig. 4*b*. One can see that qualitatively spin density distribution remains unchanged and absolute error for a_{iso} is reduced from 30 MHz for BHandHLYP functional to 19 MHz for pure Hartree-Fock method while for anisotropic part *b* only minor change of 1 MHz was found. We also note that relation between s- and p-characters in this case is greatly enhanced. In particular value of a_{iso}/b is varied from 1.66 (BHandHLYP) to 2.42 (HFX) as compared with experimental value of 2.76. On the whole one may conclude that appropriate density functional must include large fraction (~50%) of exact exchange and this is still challenge for theory.

It is worth to note that we compare calculations for 3*C*-SiC polytype with hyperfine parameters measured in 6*H*-SiC [26]. However one may expect that variation between hyperfine parameters in different polytypes is less then errors in calculated values which are caused by approximate nature of present day functionals [34].

In preceding section using total energy calculations we find no unambiguous evidence that carbon antisite may capture electron and form small polaron-like ground state. Nevertheless to proof the consistency of our calculations we performed computation of hyperfine parameters for C_{Si}^{-} for comparison with experiment as well. Corresponding results are presented in Fig. 5 and may be related to hypothetic metastable state of defect.

In Fig. 6 the spin density distributions for positive and negative carbon antisites are shown for comparison.

As one can see from Figs. 4–6 the spin density distribution for C_{Si}^{-} is qualitatively different from the one for C_{Si}^{+} center. In particular the largest hyperfine splitting corresponds to C_{Si} carbon, while for on-axis C_1 atom splitting is sufficiently large as well. This must lead to appearing of additional lines in EPR spectrum which are not observed [26]. Moreover, negative spin density on the three off-axis carbons $C_{2,3,4}$ is relatively large and may lead to observable hyperfine splitting and to further EPR spectrum complication. Thus C_{Si}^{-} model do not agree with experiment supporting conclusions made in Section 3.

We note that our calculations predict isotropic splitting of ~1 mT due to hyperfine interactions with both $Si_{1,2,3}$ and $C_{5,6,7}$ nuclei in C_{Si}^{+} shown in Fig. 6. However it is hardly may be observed because of overlapping with spectrum of another radiation defect and due to line broadening caused by ^{13}C isotope enrichment of SiC crystal [26].

Discrepancy between calculated and observed hyperfine parameters together with EPR lines broadening among other things may be caused by influence of compensating acceptors located in distant shells with respect to C_{Si}^{+}. Such mechanism was suggested for As_{Ga}^{+} antisite in GaAs [29]. Comparing results of ab initio calculations of hyperfine parameters and binding energies of defect pairs with variety of experimental data authors concluded that small deviations from tetrahedral symmetry are caused by the pairing with some other mobile defect which occurs while cooling the sample. One may suppose that similar mechanism may be valid for carbon antisite in SiC as well.

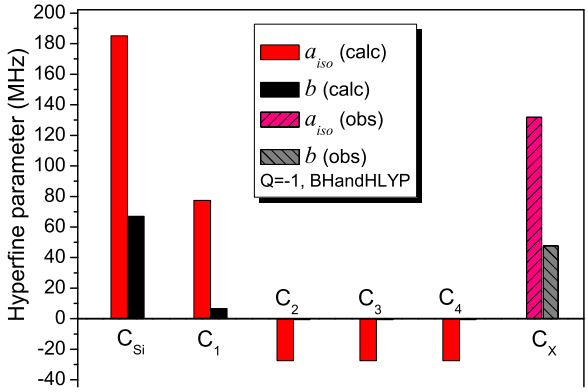

Fig. 5. Hyperfine parameters calculated using cluster approximation and BHandHLYP level of theory for C_{Si}^{-} carbon antisite. Labelling of atoms corresponds to designations in Fig. 1. Values of a_{iso}(obs) and *b*(obs) are parameters observed in [26] due to hyperfine interaction with one ^{13}C nucleus labelled as C_X.

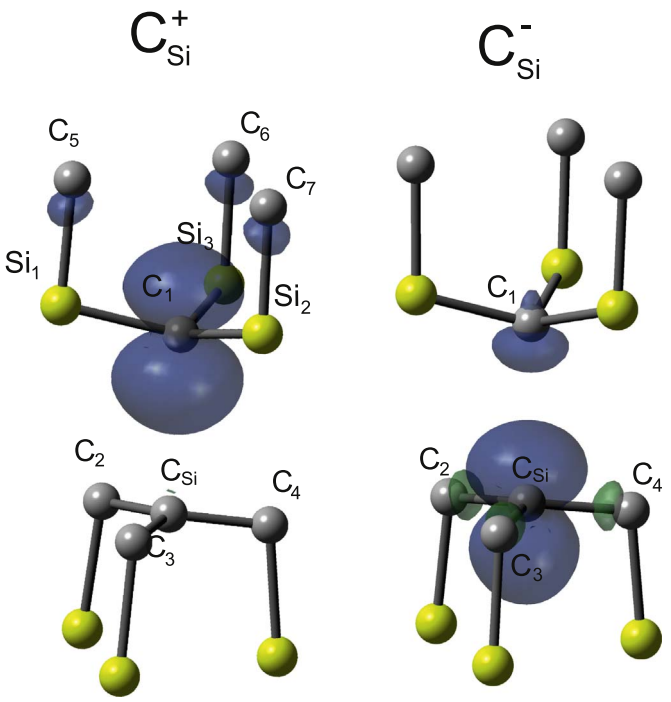

Fig. 6. Spin density distribution calculated using cluster approximation and BHandHLYP level of theory for positive (ground state) and negative (metastable state) carbon antisites in 3C-SiC. Isosurface levels correspond to 0.005 e au^{-3}. The regions with positive spin densities are marked in blue while negative spin densities on atoms C_2, C_3 and C_4 of C_{Si}^{-} center are marked in green (For interpretation of the references to color in this figure legend, the reader is referred to the web version of this article.).

5. Conclusions

The main problem associated with carbon antisite C_{Si} in SiC is whether or not it is electrically active defect which may capture electron or hole and thus manifests itself in magnetic resonance, optical and other experiments. Up till now all theoretical predictions were based on the DFT calculations utilizing local and semilocal functionals which predict the absence of electrical activity. However in [26] a new EPR spectrum with large hyperfine splitting in fast neutron irradiated and annealed ^{13}C enriched 6*H*-SiC was founded. Spin Hamiltonian parameters of this new defect differ from known parameters for a number of vacancy related centers which were well described previously by both theory and experiment. This give grounds to propose the tentative carbon antisite C_{Si}^{+} broken bond model with spin density localized on the central carbon.

In this paper we performed electronic structure calculations of positively and negatively charged carbon antisites C_{Si}^{+} and C_{Si}^{-} in 3*C*-SiC. It is well known that correct description of charge carrier localization on the defect requires elimination of the SIE. In particular this goal may be achieved with inclusion in functional a sufficient fraction of exact exchange or direct elimination of self interaction in local and semilocal functionals. Therefore we used hybrid functionals with fraction of exact exchange of 20% (B3LYP), 25% (PBE0), 50% (BHandHLYP) and 100% (HFX) together with PBE functional with SIC (Mauri-US) as well as conventional GGA BLYP and PBE functionals for comparison.

To find local and global minima and to clarify the nature of such minima we performed relaxed surface energy scans depending on the

C_{Si} - nearest carbon distance (R_{CC}) for all above mentioned Hamiltonians and both negative and positive charge states. For positively charged antisite C_{Si}^{+} one may distinguish two types of minima. The first one appears at $R_{CC} \approx 1.7$ Å and corresponds to nearly regular $C_{Si}C_{1\div4}$ tetrahedron geometry and to delocalized electronic state. The second one appears at $R_{CC} \approx 2.7$ Å and corresponds to small polaron state which is characterized by large lattice relaxation (one elongated broken C_{Si}-C_1 bond together with three shortened C_{Si}-$C_{2\div4}$ bonds). Performed calculations show that methods which sufficiently reduce the SIE (BHandHLYP, HFX and PBE+SIC) give small polaron-like ground state and vice versa - using of semilocal (BLYP, PBE) and hybrid functionals with relatively small fraction of exact exchange (B3LYP, PBE0) leads to delocalized state.

For direct comparison with EPR spectrum we performed cluster calculation of isotropic and anisotropic hyperfine parameters for central and four nearest neighbor carbons in C_{Si}^{+} antisite defect. It was shown that only for one on-axis carbon atom large hyperfine splitting must be observed. Calculated hyperfine parameters for this atom show semiquantitative agreement with experiment which is caused probably by deficiency of used BHandHLYP functional. For other four carbons (including central C_{Si} atom) hyperfine splitting is small and cannot be observed in experimental conditions used in [26].

Calculation of the ground state properties for negative carbon antisite face difficulties. Firstly, potential energy curves calculated at BHandHLYP, HFX and PBE+SIC levels of theory are qualitatively different compared to similar curves for C_{Si}^{+} (see Fig. 3). Secondly, used method of eliminating the SIE is not applicable when large effects of spin polarization are observed leading to uncertain result. Among all used density functionals only method utilizing 100% HFX and which completely neglects correlation part predicts the very small energy gain of 0.025 eV for small polaron-like ground state. However such method is known to be not sufficiently accurate while much more reliable BHandHLYP functional predicts the delocalized state. Therefore we conclude that for negative carbon antisite small polaron ground state is not realized.

Besides, in the case of C_{Si}^{-} calculated spin density distribution and hyperfine parameters are qualitatively different from the ones observed in EPR experiment. Therefore our calculations strongly support identification of EPR spectrum observed in [26] as originated from the positively charged carbon antisite. The electronic structure of this defect corresponds to self-trapped small polaron with large local lattice relaxation and broken bond configuration with spin density localized mainly on one on-axis carbon C_1 in contrast to model where spin density is localized on the central carbon C_{Si} [26]. In addition positively charged antisite model agrees well with p-type conductivity of 6H-SiC samples used in experiment.

In some sense calculation of carbon antisite in SiC faces difficulties similar to the ones for Al_{Si}^{0} impurity in quartz which was a test case for calculations during a long time. In both cases employing of popular local, semilocal and hybrid functionals do not lead to proper hole localization until self interaction correction was explicitly included in calculations.

Based on the performed analysis we may predict that carbon antisite is a difficult case for calculation of (0/+) transition energy level in the gap. Indeed, the C_{Si}^{+} defect is isoelectronic with the recently investigated neutral B_{Si} center in SiC [34]. Similar to carbon antisite the B_{Si}^{0} center induces three short B-C bonds and one elongated B-C bond. This leads to the extremely large finite size effects for neutral supercell due to defect-induced elastic strains [34]. In the case of C_{Si}^{+} we expect even stronger effect because lattice relaxation in the vicinity of antisite is larger as compared to the neutral boron impurity.

In conclusion presented calculations together with experimental findings [26] give some evidence that experimentally detectable isolated carbon antisite defect may be created in SiC by means of defect engineering methods in addition to a number of other known intrinsic defects. Nevertheless we cannot exclude that in real crystal C_{Si} defect may be a part of some complex where spin density is modified leading to deviation of calculated hyperfine parameters from observed in experiment [26]. In this case performed calculations of electronic structure of isolated antisite are necessary for correct determination of binding energy, thermal stability and kinetics of complex formation.

Acknowledgments

Authors acknowledges the financial support and access to the computational cluster of Kyiv Institute of Semiconductor Physics of the National Academy of Sciences of Ukraine (Grant No. III-9-12).

References

[1] H. Hausmann, A. Pillukat, P. Ehrhart, Phys. Rev. B 54 (1996) 8527.
[2] T. Mattila, R.M. Nieminen, Phys. Rev. Lett. 74 (1995) 2721.
[3] J.R. Weber, W.F. Koehl, J.B. Varley, A. Janotti, B.B. Buckley, C.G.V. de Walle, D.D. Awschalom, J. Appl. Phys. 109 (2011) 102417.
[4] W.F. Koehl, B.B. Buckley, F.J. Heremans, G. Calusine, D.D. Awschalom, Nature 479 (2011) 84.
[5] A.L. Falk, B.B. Buckley, G. Calusine, F. Koehl, V.V. Dobrovitski, A. Politi, C.A. Zorman, P.X.-L. Feng, D.D. Awschalom, Nat. Commun. 4 (2013) 1819.
[6] J. Isoya, T. Umeda, N. Mizuochi, N.T. Son, E. Janzén, T. Ohshima, Phys. Stat. Sol. B 245 (2008) 1298.
[7] P.G. Baranov, A.P. Bundakova, A.A. Soltamova, Phys. Rev. B 83 (2011) 125203.
[8] T.C. Hain, F. Fuchs, V.A. Soltamov, P.G. Baranov, G.V. Astakhov, T. Hertel, V. Dyakonov, J. Appl. Phys. 115 (2014) 133508.
[9] M. Bockstedte, A. Gali, A. Mattausch, O. Pankratov, J.W. Steeds, Phys. Stat. Sol. B 245 (2008) 1281.
[10] T. Wimbauer, B.K. Meyer, A. Hofstaetter, A. Scharmann, H. Overhof, Phys. Rev. B 56 (1997) 7384.
[11] T. Umeda, Y. Ishitsuka, J. Isoya, N.T. Son, E. Janzén, N. Morishita, T. Ohshima, H. Itoh, A. Gali, Phys. Rev. B 71 (2005) 193202.
[12] T. Umeda, J. Isoya, N. Morishita, T. Ohshima, T.K.A. Gali, P. Deák, N.T. Son, E. Janzén, Phys. Rev. B 70 (2004) 235212.
[13] V.Y. Bratus', T.T. Petrenko, S.M. Okulov, T.L. Petrenko, Phys. Rev. B 71 (2005) 125202.
[14] T.T. Petrenko, T.L. Petrenko, V.Y. Bratus', J. Phys.: Condens. Matter 14 (2002) 12433.
[15] T. Umeda, J. Isoya, N. Morishita, T. Ohshima, E. Janzén, A. Gali, Phys. Rev. B 79 (2009) 115211.
[16] N.T. Son, P. Carlsson, J. ul Hassan, E. Janzén, T. Umeda, J. Isoya, A. Gali, M. Bockstedte, N. Morishita, T. Ohshima, H. Itoh, Phys. Rev. Lett. 96 (2006) 055501.
[17] T. Umeda, N.T. Son, J. Isoya, E. Janzén, T. Ohshima, N. Morishita, H.I.A. Gali, M. Bockstedte, Phys. Rev. Lett. 96 (2006) 145501.
[18] F. Bruneval, G. Roma, Phys. Rev. B 83 (2011) 144116.
[19] C. Wang, J. Bernholc, R.F. Davis, Phys. Rev. B 38 (1988) 12752.
[20] L. Torpo, S. Pöykkö, R.M. Nieminen, Phys. Rev. B 57 (1998) 6243.
[21] F. Bechstedt, A. Fissel, J. Furthmüller, U. Grossner, A. Zywietz, J. Phys.: Condens. Matter 13 (2001) 9027.
[22] L. Torpo, M. Marlo, T.E.M. Staab, R.M. Nieminen, J. Phys.: Condens. Matter 13 (2001) 6203.
[23] F. Bernardini, A. Mattoni, L. Colombo, Eur. Phys. J. B 38 (2004) 437.
[24] A. Gali, P. Deák, P. Ordejón, N.T. Son, E. Janzén, W.J. Choyke, Phys. Rev. B 68 (2003) 125201.
[25] A. Gali, P. Deák, N.T. Son, E. Janzén, Phys. Rev. B 71 (2005) 035213.
[26] P.G. Baranov, I.V. Ilyin, A.A. Soltamova, E.N. Mokhov, Phys. Rev. B 77 (2008) 085120.
[27] D.J. Chadi, K.J. Chang, Phys. Rev. Lett. 60 (1988) 2187.
[28] D.J. Chadi, Phys. Rev. B 68 (2003) 193204.
[29] H. Overhof, J.M. Spaeth, Phys. Rev. B 72 (2005) 115205.
[30] A.J. Cohen, P. Mori-Sánchez, W. Yang, Science 321 (2008) 792.
[31] A.J. Cohen, P. Mori-Sánchez, W. Yang, Chem. Rev. 112 (2012) 289.
[32] J.P. Perdew, A. Ruzsinszky, G.I. Csonka, O.A. Vydrov, G.E. Scuseria, V.N. Staroverov, J. Tao, Phys. Rev. A 76 (2007) 040501 (R).
[33] P. Mori-Sánchez, A.J. Cohen, W. Yang, Phys. Rev. Lett. 100 (2008) 146401.
[34] T.T. Petrenko, T.L. Petrenko, Phys. Rev. B 93 (2016) 165203.
[35] S. Sicolo, G. Palma, C.D. Valentin, G. Pacchioni, Phys. Rev. B 76 (2007) 075121.
[36] S. Lany, Phys. Status Solidi B 248 (2011) 1052.
[37] M. d'Avezac, M. Calandra, F. Mauri, Phys. Rev. B 71 (2005) 205210.
[38] J. VandeVondelle, M. Krack, F. Mohamed, M. Parrinello, T. Chassaing, J. Hutter, Comput. Phys. Commun. 167 (2005) 103.
[39] G. Lippert, J. Hutter, M. Parrinello, Theor. Chem. Acc. 103 (1999) 124.
[40] J. VandeVondele, J. Hutter, J. Chem. Phys. 127 (2007) 114105.
[41] S. Goedecker, M. Teter, J. Hutter, Phys. Rev. B 54 (1996) 1703.
[42] M. Guidon, J. Hutter, J. VandeVondele, J. Chem. Theory Comput. 5 (2009) 3010.
[43] M. Guidon, J. Hutter, J. VandeVondele, J. Chem. Theory Comput. 6 (2010) 2348.
[44] F. Neeze, Wiley Interdiscip. Rev.: Comput. Mol. Sci. 2 (2012) 73.
[45] F. Weigend, R. Ahlrichs, Phys. Chem. Chem. Phys. 7 (2005) 3297.
[46] F. Neese, F. Wennmohs, A. Hansen, U. Becker, Chem. Phys. 356 (2009) 98.
[47] F. Weigend, Phys. Chem. Chem. Phys. 8 (2006) 1057.
[48] F. Neese, Coord. Chem. Rev. 253 (2009) 526.